82. Flash Photolysis of 5-Methyl-1,4-naphthoquinone in Aqueous Solution: Kinetics and Mechanism of Photoenolization and of Enol Trapping

by **Yvonne Chiang** and **A. Jerry Kresge***

Department of Chemistry, University of Toronto, Toronto, Ontario M5S 3H6, Canada

and **Bruno Hellrung, Patrick Schünemann,** and **Jakob Wirz***

Institut für Physikalische Chemie der Universität Basel, Klingelbergstrasse 80, CH-4056 Basel

Dedicated to our colleague *Fabian Gerson* who is venturing to new shores

(4.IV.97)

5-Methyl-1,4-naphthoquinone (**1**) is a remarkable probe to study hydrogen and proton transfer reactions. The photoenol 4-hydroxy-5-methylidene naphthalen-1(5*H*)-one (**2**) is formed in the ground state within 2 ps of excitation and with a quantum yield of unity, presumably through a conical intersection of the S_0 and S_1 hypersurfaces. In aqueous acid, enol **2** is hydrated to 5-(hydroxymethyl)naphthalene-1,4-diol **3** (X = OH, *Scheme 1*). The rate of hydration of **2** increases linearly with acid concentration from *ca.* 1.5×10^4 s^{-1} at pH 6 to reach a maximum value of 9×10^7 s^{-1} when the remaining carbonyl function is protonated, $pK_a(\mathbf{2}^+) = 1.1$. Contrary to an earlier suggestion, the rate-determining step in the acid-catalyzed hydration of **2** is addition of water to the conjugate acid $\mathbf{2}^+$. Pronounced acceleration of the decay rate of **2** by hydrazoic-acid buffers indicates competitive trapping of $\mathbf{2}^+$ by the azide ion. In neutral-to-weakly-basic solutions, enol **2** reacts by ionization, $pK_a(\mathbf{2}) = 6.5$, and nearly diffusion-controlled condensation of the carbanionic species $\mathbf{2}^-$ with quinone **1**. Protonation at the methylidene C-atom does not compete measurably with protonation on carbonyl O-atom, despite a substantial thermodynamic bias for carbon protonation of *ca.* 50 kJ mol^{-1} for **2**, and 100 kJ mol^{-1} for $\mathbf{2}^-$.

Introduction. – Photoenolization of 5-methyl-1,4-naphthoquinone (**1**) generates the amphoteric enol 4-hydroxy-5-methylidenenaphthalen-1(5*H*)-one (**2**) which forms the carbocationic intermediate $\mathbf{2}^+$ in acid and the carbanionic intermediate $\mathbf{2}^-$ in base (*Scheme 1*). Twenty years ago, we reported that the photoenol **2** was trapped by protonation and subsequent capture of the carbocationic species $\mathbf{2}^+$ so formed; with glacial AcOH as the trapping agent, this provided the acetate derivative **3** (X = AcO) [1]. *Chatterjee* and *Rokita* have used a derivative of **1** to achieve light-induced, sequence-specific alkylation of DNA [2].

The present work was done to address three questions: *i*) Is the photoenol of **1** formed adiabatically in an excited state, as was shown to be the case for 1-methylanthraquinone [3] and *o*-methylacetophenone [4]? *ii*) Is proton transfer to the carbonyl O-atom of **2** indeed slower than the subsequent attack of the nucleophile on the C-atom, as was proposed earlier [1]? We now provide conclusive evidence to the contrary. *iii*) Photoenol **2** contains both strongly basic methylidene C- and weakly basic carbonyl O-functionalities. Proton transfer to C-atoms is in general much slower than proton transfer to N- or O-atoms. Is the thermodynamic bias in favor of *C*-protonation sufficient to make it kinetically competitive with *O*-protonation?

Scheme 1

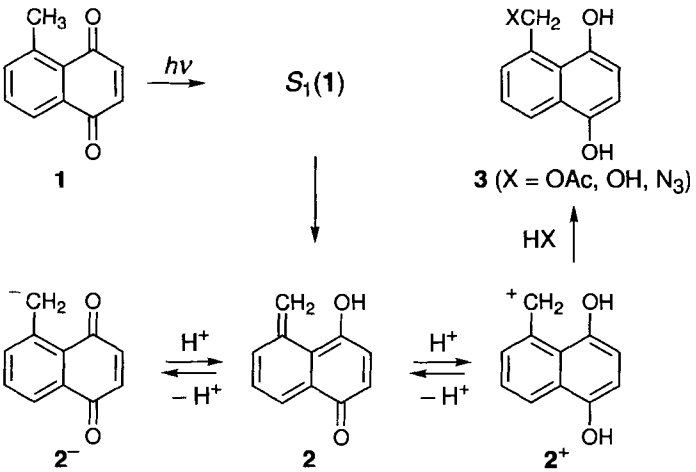

Results. – *Continuous Irradiation, Products, and Quantum Yields.* Solutions of **1** (1×10^{-4} M) in dilute aqueous $HClO_4$ were irradiated with monochromatic light of either 313 or 365 nm. The reaction progress was monitored by UV spectroscopy (*Fig. 1*) which indicated rapid and quantitative conversion to the expected photoproduct, 5-(hydroxymethyl)naphthalene-1,4-diol (**3**, X = OH). The absorption spectrum of **3** (X = OH) was very similar to that of naphthalene-1,4-diol [1] and changed to that of the conjugate dianion when strong base was added. Attempts to isolate **3** (X = OH) failed due to facile dehydration (*Exper. Part*): GC/MS analysis of **1**, and of the product obtained after

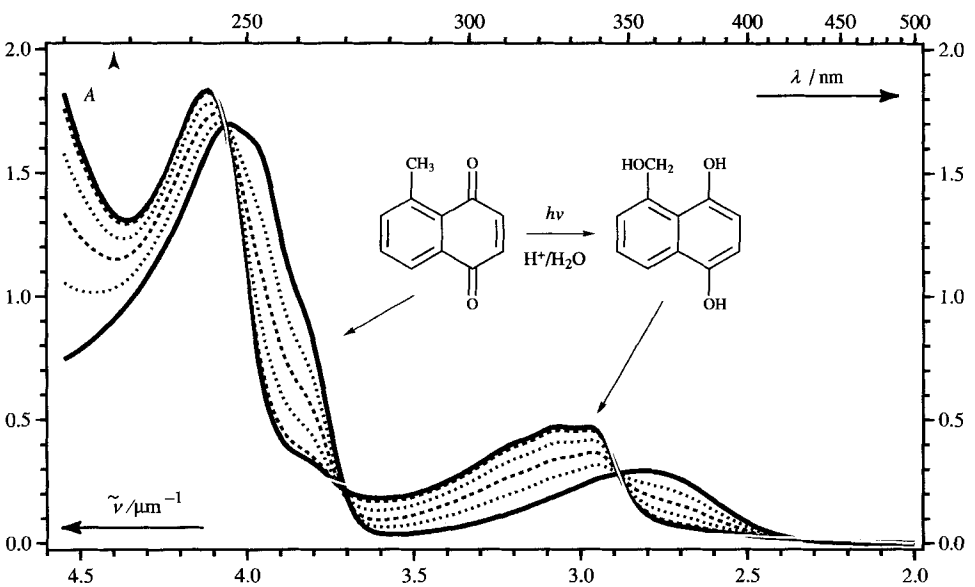

Fig. 1. *Spectrophotometric changes observed during the photohydration of* **1**

complete conversion of **1** by exhaustive photolysis at 365 nm in 0.01N aqueous HCl, gave identical results due to immediate dehydration of **3** (X = OH) in the injection chamber. The equally labile photoproduct **3** (X = AcO), obtained earlier by irradiation of **1** in AcOH, had been identified by derivatization [1]. The mass spectrum of the product obtained by irradiation of **1** in acidic D_2O was also nearly identical with that of **1**, *i.e.*, hardly any D-atoms had been incorporated (< 3%). Exchange of deuterated alcohol functions of **3** (X = OD) probably took place by exposure to adventitious moisture during workup. The result is, nevertheless, important to show that D addition to the methylidene group of **2**, which would have formed the hydrate deuterated at a nonexchangeable position, does not occur (see the *Discussion*).

The photohydration quantum yield of **1** in aqueous $HClO_4$, ϕ_{hydr}, was unity within experimental error (± 10%) for acid concentrations ranging from 0.001 to 1M. In neutral and weakly basic solutions, **1** was consumed with even higher quantum yield, $\phi_{rxn} \approx 2$, and a different, complex mixture of photoproducts (absorption onset at 350 nm, shoulder at 315 nm) was formed. GC/MS and ^{1}H-NMR analysis indicated the presence of products formed by condensation of **2** and **1** that were not further identified.

Nanosecond Flash Photolysis. Flash photolysis of solutions of **1** in dilute aqueous $HClO_4$ (0.001–0.010M) with a 25-ns laser pulse at either 248 or 351 nm gave immediate and strong transient absorbance in the range of 550 to 700 nm, λ_{max} = 620 nm (*Fig. 2*, curve *a*). This photoproduct is persistent in a rigid glass at 77 K and was previously identified as photoenol **2** [1]; that assignment was based on trapping experiments with AcOH, the characteristic sensitivity of the reketonization rate to H-bond acceptor properties of the solvent, and the agreement of the remarkably long-wavelength absorption with calculations. The decay of **2** was monitored at 620 nm. Excellent fits to the ab-

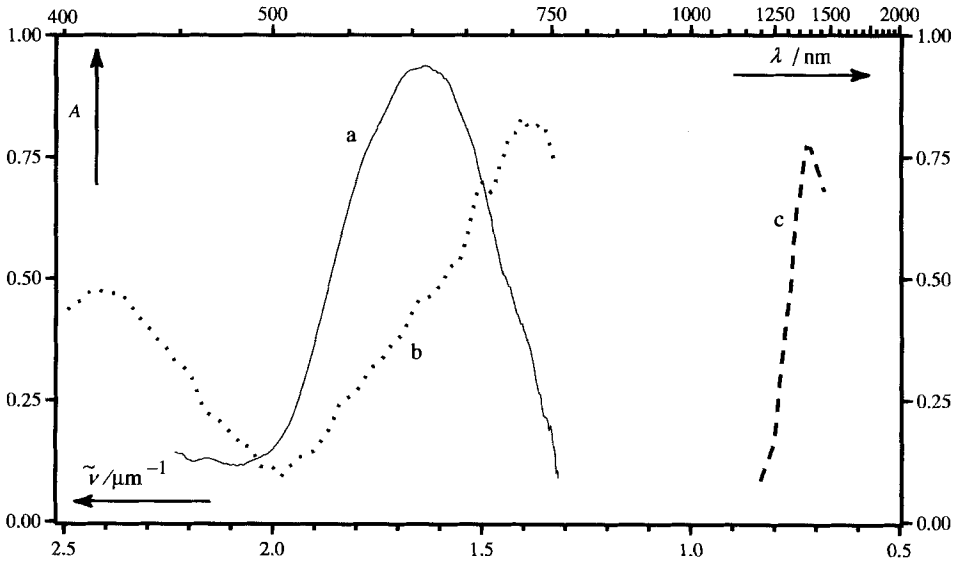

Fig. 2. *Transient absorption spectra of* a) **2** *in 0.001N* $HClO_4$ (———), b) $\mathbf{2}^+$ *in 1N* $HClO_4$ (···), *and* c) $\mathbf{2}^-$ *in 0.001N* NaOH (– – – –) *determined by ns spectrographic flash photolysis* (248 nm) *of* **1**

sorbance decay traces were obtained by nonlinear least-squares analysis using a single exponential decay function. The observed rate constants are collected in *Table 1*.

Table 1. *Observed First-Order Decay Rates of Enol* **2** *in Acidic Aqueous Solutions* (25°)

$[H^+]$/M	$k_{obs}/(10^6\ s^{-1})$[a])	No. of measurements	Instrument[b])
1.13×10^{-4} (AcOH)	0.0203 ± 0.0005	30	μs
5.3×10^{-5} (HN_3)	0.042 ± 0.002[c])	16	ns
1.55×10^{-4} (HCO_2H)	0.207 ± 0.005[c])	15	ns
0.001	1.12 ± 0.07	6	ns
0.002	2.27 ± 0.04	4	ns
0.004	4.45 ± 0.08	4	ns
0.007	7.58 ± 0.08	4	ns
0.010	10.7 ± 0.5	5	ns
0.020	20.5 ± 0.6	4	ns
0.040	34 ± 3	4	ns
0.050	35 ± 3	5	ns
0.070	48 ± 3	4	ns
0.100	54 ± 6	10	ns
0.100	44 ± 6	3	ps
0.250	59 ± 3	4	ns
0.500	61 ± 2	4	ns
1.000	62 ± 14	5	ps
1.000	100 ± 30	3	ps-spec

[a]) Errors are standard errors of the sample means. All measurements, except the ones with > 0.1N $HClO_4$, were done with solutions of ionic strength $I = 0.1$N.

[b]) μs: excitation with a conventional discharge flash lamp. ns: excitation with 20-ns excimer laser pulse. ps: excitation with 0.8 ps laser pulse, kinetic monitoring was performed with a grating monochromator and a photomultiplier tube. ps-spec: spectrographic monitoring with pump-probe technique.

[c]) Intercepts determined by linear extrapolation of buffer dilution plots.

Photoenolization of **1** also took place at pH > 3, but in neutral and basic solutions the decay kinetics of enol **2** was more complex. It was essential to use solutions freshly prepared in the dark and to expose them only to a single flash. The instability of naphthoquinones to aqueous base required fresh solutions, and the preparation time of 1 min limited practical work to pH < 10. The exclusion of light was essential because flash photolysis of the photoproducts generated secondary transient intermediates absorbing at the same wavelengths as **2**. In spite of these precautions, the transient decays at pH > 5 did not obey the first-order rate law cleanly. Deviations from first-order decays were particularly pronounced at pH ≥ 7 and in dilute solutions of **1**. The half-life of the transient absorbance decreased with increasing initial concentrations of quinone **1**, indicating very rapid (*ca.* $5 \times 10^9\ M^{-1}s^{-1}$) attack of enolate ion $\mathbf{2}^-$ on remaining quinone **1**. It is then no surprise that the observed kinetics were of mixed order in dilute solutions, because the reagents of the bimolecular reaction, $\mathbf{2}^-$ and **1**, were present in comparable concentrations: exactly equal concentrations would have produced a second-order decay trace, whereas a large excess of reactant **1** would give rise to first-order decay traces with observed rate constants proportional to the concentration of **1**.

Buffer Dilution Plots. Rates of trapping of the photoenol **2** were measured in aqueous formic- and hydrazoic-acid buffer solutions. Solutions of constant buffer ratio and constant ionic strength ($I = 0.10$M maintained by addition of $NaClO_4$), but variable total buffer concentrations were used. H^+-Ion concentrations consequently remained constant along a given buffer solution series. Catalysis by hydrazoic-acid buffer at a buffer ratio $[HN_3]/[NaN_3]$ of 2:3 was quite pronounced. A buffer dilution plot with total buffer concentrations in the range of $(0.25-1.00)\times10^{-2}$ M was linear with a slope $k_{HN_3} = (4.42 \pm 0.47)\times10^6\ M^{-1}\ s^{-1}$ against HN_3 concentration and with an intercept of $(4.17 \pm 0.21)\times10^4\ s^{-1}$. Buffer catalysis by HCO_2H buffer was just barely significant for total buffer concentrations in the range of 0.06–0.15M at a buffer ratio $[HCO_2H]/[HCO_2Na] = 0.55$, $k_{obs}/s^{-1} = (2.07 \pm 0.05)\times10^5 + (4.25 \pm 1.35)\times10^5$ $[HCO_2H]$. Buffer catalysis was no longer detectable in AcOH buffer for total buffer concentrations in the range of 0.01–0.10M at a buffer ratio $[HAc]/[NaAc] = 0.42$, $k_{obs} = (2.03 \pm 0.05)\times10^4\ s^{-1}$. H^+-Ion concentrations of $[H^+] = 1.55\times10^{-4}$ M (HCO_2H), $[H^+] = 2.37\times10^{-5}$ M (HN_3) and $[H^+] = 1.13\times10^{-5}$ M (AcOH) were calculated using the thermodynamic acidity constants $pK_a^\ominus$ (HCO_2H) = 3.75 [5a], $pK_a^\ominus(HN_3) = 4.65$ [6], $pK_a^\ominus$ (AcOH) = 4.76 [5b] and activity coefficients, $\gamma_{(H^+)} = 0.83$, $\gamma_{(AcO^-)} = 0.775$, and $\gamma_{(HCOO^-)} = \gamma_{(N_3^-)} = 0.76$, recommended by *Bates* [7] for ionic strength $I = 0.1$M.

Picosecond Flash Photolysis. Transient absorbance changes on the ps time scale were determined by pump-probe spectrographic flash photolysis with a 248-nm excitation pulse of 0.8 ps duration. Neutral aqueous solutions were prepared by addition of 20% MeCN as a cosolvent to achieve a concentration of **1** (2.5×10^{-4} M) with optimal absorbance at the excitation wavelength of 248 nm ($A = 0.5$ over a path length of 1 mm). A series of spectra was taken with delays increasing in increments of 0.3 ps up to a delay 20 ps after the pump pulse, and of 10 ps up to 1.9 ns. The build-up of the strong absorption of **2** in the visible, $\lambda_{max} = 620$ nm, was essentially complete within 2 ps. Spectral changes that may reflect the photoenolization process and/or thermal relaxation of the photoenol were observed during the first 2 ps after the peak of the excitation flash, but these were close to the time resolution of our setup. To estimate the rate of singlet-triplet intersystem crossing of **1**, parent 1,4-naphthoquinone in the same solvent mixture was used as a benchmark: formation of the triplet-triplet absorption of 1,4-naphthoquinone ($\lambda_{max} = 365$ nm [8], *Fig. 3*, curve *a*) was clearly resolved with a rate of $(1.1 \pm 0.2)\times10^{11}\ s^{-1}$. Photoenolization of **1** is at least five times as fast.

The solubility of **1** in aqueous $HClO_4$ was sufficient to achieve the required concentration of 2.5×10^{-4} M of **1** without the addition of any cosolvent. Singular value decomposition [9] of a series of spectra that were obtained with 1N aqueous $HClO_4$ and in the time range of 2 ps to 2 ns after the pump pulse indicated the presence of three significant spectral components. Kinetic analysis of the pump-probe spectra was limited to the spectral range of 310 nm $\leq \lambda \leq$ 430 nm to avoid interference with the absorption of solvated electrons at longer wavelengths. The latter were formed by two-photon ionization of H_2O and were also observed without solute **1**; they were scavenged by protons with a rate of $k = 1\times10^{11}\ M^{-1}\ s^{-1}$. Formation of photoenol **2** was again complete within a few ps.

Enol **2** was then converted to a new transient intermediate that is attributed to protonated photoenol $\mathbf{2}^+$. This conversion obeyed a first-order rate law and its rate coefficient was proportional to acid concentration, $k_{(H^+)} = (1.6 \pm 0.5)\times10^{10}\ M^{-1}\ s^{-1}$ (*Fig. 4*).

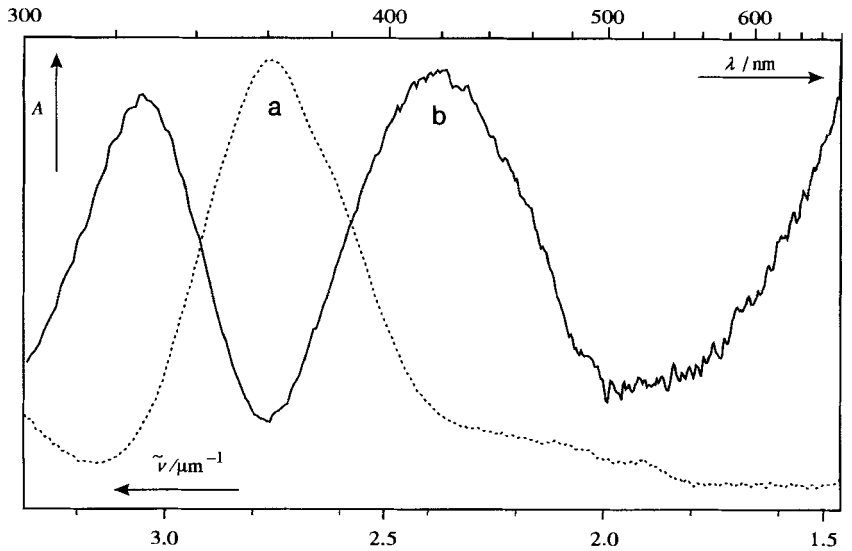

Fig. 3. *Transient absorption spectra observed by ps pump-probe spectroscopy using a 0.8-ps pump pulse at 248 nm. a*) Absorption spectrum of triplet 1,4-naphthoquinone in MeCN, 70-ps delay after excitation of 1,4-naphthoquinone (·····). *b*) Transient absorption of $\mathbf{2}^+$, 300-ps delay after excitation of **1** in 1M $HClO_4$ (———).

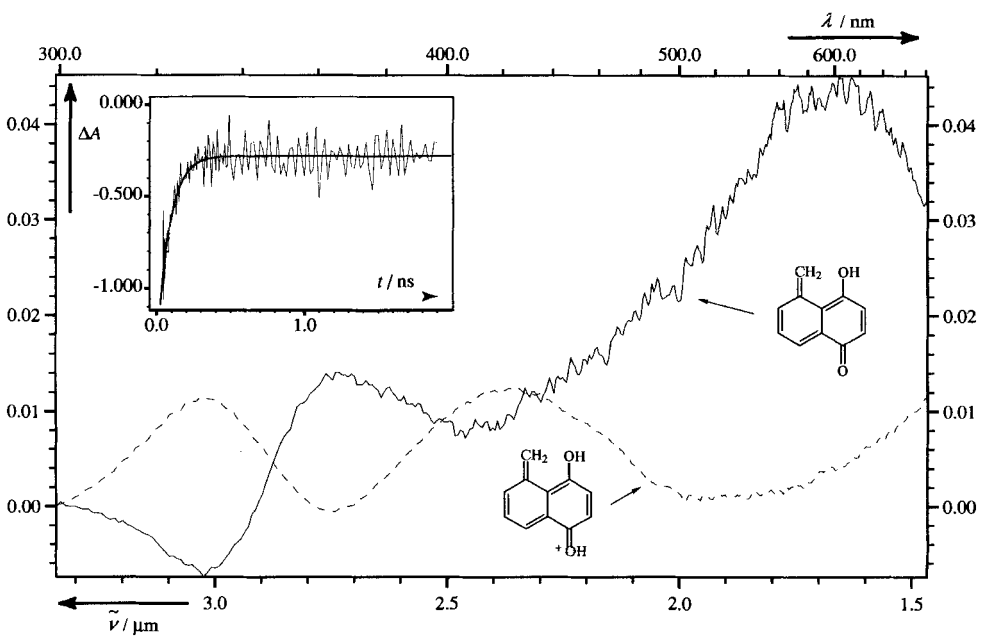

Fig. 4. *Transient absorption spectra* of **2** *and* $\mathbf{2}^+$ *in* 1N $HClO_4$ *determined by pump-probe spectroscopy.* The inset shows the temporal buildup of $\mathbf{2}^+$ from **2** as defined by the loading coefficients of the first eigenspectrum determined by factor analysis of the complete set of spectra.

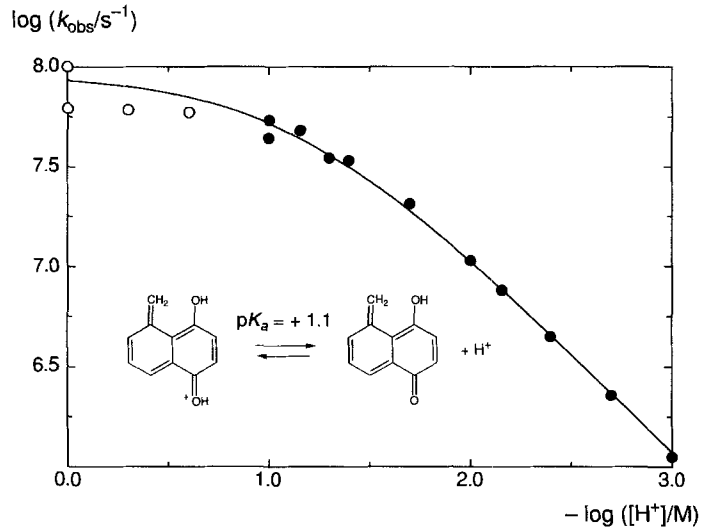

Fig. 5. *pH Rate profile of the acid-catalyzed hydration of* **2**. The data obtained by ns flash photolysis (•) were analyzed by nonlinear least-squares fitting of the logarithmic form of *Eqn. 2*. The data shown as empty circles (o) were not included in the analysis.

The transient spectrum of $\mathbf{2}^+$ observed with delays > 300 ps after the laser pulse, *i.e.*, after the solvated electrons had completely disappeared, is shown in *Fig. 3*, curve *b*; it agrees well with that observed as the primary intermediate by spectrographic flash photolysis of strongly acidic solutions on the ns apparatus (*Fig. 2*, curve *b*). Global analysis of a series of transient spectra recorded up to a maximum delay of 19 ns indicated a decay rate of *ca.* $1 \times 10^8\ s^{-1}$ for $\mathbf{2}^+$ at $[HClO_4] = 1$M. The decay of $\mathbf{2}^+$ was also determined by monitoring the transient absorbance changes at 430 nm with a photomultiplier, using the subpicosecond laser pulse for excitation. The risetime of this detection system was 1.5 ns. Several hundred shots were accumulated to improve the signal-to-noise ratio. Such measurements gave $k_{obs} = (6.2 \pm 1.4) \times 10^7\ s^{-1}$ for the decay rate of $\mathbf{2}^+$ in 1N $HClO_4$ and $k_{obs} = (4.4 \pm 0.6) \times 10^7\ s^{-1}$ for 0.1N $HClO_4$.

Analysis of the pH Rate Profile. The first-order rate coefficients for the decay of enol **2**, k_{obs}, were directly proportional to acid concentration in dilute $HClO_4$ solutions, but saturation of acid catalysis became apparent at acid concentrations exceeding 0.02M (*Table 1* and *Fig. 5*). Such behavior is characteristic for reactions proceeding through a protonation preequilibrium [10], followed, in this case, by rate-determining hydration of the protonated enol $\mathbf{2}^+$ (*Eqn. 1*).

$$\mathbf{2} + H^+ \underset{k_{(-H^+)}}{\overset{k_{(H^+)}}{\rightleftharpoons}} \mathbf{2}^+ \xrightarrow{k_0} \mathbf{3} \qquad (1)$$

The ratio of the rate constants of ionization of $\mathbf{2}^+$ and protonation of **2**, $k_{(-H^+)}/k_{(H^+)}$, is equal to the acidity constant of the protonated enol $\mathbf{2}^+$, $K_a(\mathbf{2}^+)$, and, provided that $k_{(-H^+)} \gg k_0$, the rate law for hydration of **2** according to the mechanism of *Eqn. 1* is first-order with a pH-dependent rate coefficient k_{obs} given by *Eqn. 2*.,

$$k_{obs} = \frac{k_0}{[H^+] + K_a(2^+)}[H^+], \quad (2)$$

that simplifies to $k_{obs} = k_0$ for $[H^+] >> K_a(2^+)$ and to $k_{obs} = k_0[H^+]/K_a(2^+)$ for $[H^+] << K_a(2^+)$.

The standard errors of rate constants determined by flash photolysis are approximately proportional to their absolute values, *i.e.*, errors in $\log(k_{obs})$ are constant. Therefore, analysis was done by nonlinear least-squares fitting of the logarithmic form of *Eqn. 2* using data points determined with aqueous $HClO_4$ solutions (0.001–0.100N) (*Table 1*). A good fit was obtained with the parameters $k_0 = (9.4 \pm 0.8) \times 10^7\ s^{-1}$ and $K_a = (0.079 \pm 0.009)$M, $pK_a = 1.10 \pm 0.05$ (*Fig. 5*). The intercepts of the buffer dilution plots (*Table 1*) are somewhat larger than the values calculated by extrapolation of *Eqn. 2*. The deviations increased with increasing pH of the buffers and reached 56% in AcOH buffer. These deviations are attributed to increasing contributions of the condensation reaction proceeding from the enol anion $\mathbf{2}^-$ (*vide supra*).

We were concerned that the lifetimes determined in the most acidic solutions were on the order of 20 ns, and that the apparent saturation of acid catalysis might have been due to a systematic error, since the pulse width of the exciting laser pulse was of the same order of magnitude. The data obtained with ps time resolution clearly show that this is not the case. These values are 30 and 16% smaller, respectively, than those predicted by extrapolation of the data obtained by ns flash photolysis using *Eqn. 2*. The difference found in 1N $HClO_4$ may, in part, be attributed to the increased ionic strength. We attribute the 16% discrepancy between the two values obtained at $[HClO_4] = 0.1$M to the lower accuracy of the ps setup for measurements in the time domain of 10 ns. The data obtained with the ps setup were, therefore, not included for the fitting of *Eqn. 2*. Nevertheless, these measurements are important to prove that the saturation of acid catalysis observed by ns flash photolysis is not an artifact arising from limitations in time resolution.

Nonexponential decays were observed in neutral-to-basic solutions. Rate constants obtained by forcing first-order fits to the complex decays followed a V-shaped pH profile with a minimum of *ca.* $1.5 \times 10^4\ s^{-1}$ at pH 5.5. In basic solutions the decay rates rose again, but rapidly reached their maximum value of *ca.* $5 \times 10^4\ s^{-1}$, indicating ionization of **2** around pH 6.7. Accurate determination of the dissociation constant of enol **2** from the kinetic data was not attempted.

Titration of the Photoenol in Aqueous Acid and Base by Nanosecond Spectrographic Flash Photolysis. Another manifestation of the protolytic equilibria of enol **2** are the accompanying changes in the transient absorption spectra. The shifts of the first absorption band of **2** upon protonation to the conjugate acid $\mathbf{2}^+$, and deprotonation to the conjugate base $\mathbf{2}^-$ (*Fig. 2*), agree well with those predicted by simple PPP SCF SCI calculations (*Table 2*). These changes provide an alternative method to determine the equilibrium constants of protonation and ionization of **2** in aqueous solution.

Aqueous $HClO_4$ (0.001–0.100N $HClO_4$) was used to titrate the protonation of **2**. Ionic strength was adjusted to $I = 0.1$M by addition of $NaClO_4$. Transient spectra were recorded in the wavelength range from 450 to 750 nm and in time windows of 20 ns with almost zero delay to the maximum of the ns laser pulse. Three to five transient spectra were averaged for each acid concentration. The spectra so obtained were collected in a

Table 2. *Results of PPP SCF CI Calculations and Experimental Data for the Absorption Spectra of the Photoenol* **2**, *Its Protonated Form* $\mathbf{2}^+$, *and Its Anion* $\mathbf{2}^-$

Compound	Calculated		Observed	
	λ/nm	osc. strength f	λ_{max}/nm	rel. intensity
	579	0.59	620	1
2	369	0.07	360	0.3
	342	0.07		
	714	0.23	720	1
$\mathbf{2}^+$	423	0.21	415	0.5
$\mathbf{2}^-$	1033	0.16	1300	

data matrix and subjected to factor analysis. Two components were sufficient to reproduce all spectra within experimental accuracy. Enol **2** was only about half-protonated in 0.1N $HClO_4$. Ionization ratios at higher acid concentrations were not included in the analysis to obviate the need to determine an appropriate acidity function, but a spectrum recorded with 1N $HClO_4$ was used to define the end-point spectrum of the protonated enol $\mathbf{2}^+$ and, thereby, to determine the relative concentrations $[\mathbf{2}]_{rel}$ at various acid concentrations of $[H^+]$ from the loading coefficients determined by singular value decomposition of the spectral data matrix [11]. Nonlinear least-squares fitting of the concentration quotient, $K_a(\mathbf{2}^+) = [H^+][\mathbf{2}]/[\mathbf{2}^+]$, to these data points gave $pK_a(\mathbf{2}^+) = 1.01 \pm 0.10$ (*Fig. 6, a*). This value is in satisfactory agreement with that determined independently from the pH-rate profile, $pK_a(\mathbf{2}^+) = 1.10 \pm 0.05$. In *Table 3* we quote the weighted mean of these values as our best estimate of the dissociation quotient of the protonated enol, $pK_a(\mathbf{2}^+) = 1.08 \pm 0.04$.

The second ionization constant, $K_a(\mathbf{2}) = [H^+][\mathbf{2}^-]/[\mathbf{2}]$, was determined by fitting a titration curve, *Eqn. 3*,

$$A_{0,obs} = \frac{A_0(\mathbf{2})[H^+] + A_0(\mathbf{2}^-)K_a(\mathbf{2})}{[H^+] + K_a(\mathbf{2})} \tag{3}$$

to the initial absorbance $A_{0,obs}$ measured at 610 nm on a conventional (μs) kinetic flash photolysis setup with buffered solutions (*Fig. 6, b*). $A_0(\mathbf{2})$ and $A_0(\mathbf{2}^-)$ are the initial absorbances at 610 nm of **2**, measured at pH $\ll pK_a(\mathbf{2})$, and of $\mathbf{2}^-$, measured at pH $\gg pK_a(\mathbf{2})$, respectively. Acetate buffers ($c_{tot} = 0.025$M) were used to adjust acid concentration in the pH range 5.00–5.75 and phosphate buffers ($c_{tot} = 0.025$M) for 5.98–7.50. Ionic strength was adjusted to $I = 0.1$M by addition of NaCl. Proton concentrations of the solutions were measured with a calibrated glass electrode [12] for control purposes; measured values were within $\pm$ 0.02 pH units of those calculated from the buffer ratio using thermodynamic dissociation constants from the literature, $pK_a^{\ominus}(AcOH) = 4.76$ [13], $pK_a^{\ominus}(H_2KPO_4) = 7.20$ [14], and activity coefficients, $\gamma_{(H^+)} = 0.83$, $\gamma_{(AcO^-)} = \gamma_{(H_2PO_4^-)} = \gamma_{(K^+)} = 0.775$ and $\gamma_{(HPO_4^{2-})} = 0.355$, recommended by *Bates* [7]. This procedure gave $pK_a(\mathbf{2}) = 6.45 \pm 0.04$.

Kinetic Isotope Effect. Some measurements of the decay rate of **2** were also performed with D_2O solutions of DCl and $DClO_4$ at nominal concentrations of 0.001M and 0.006M,

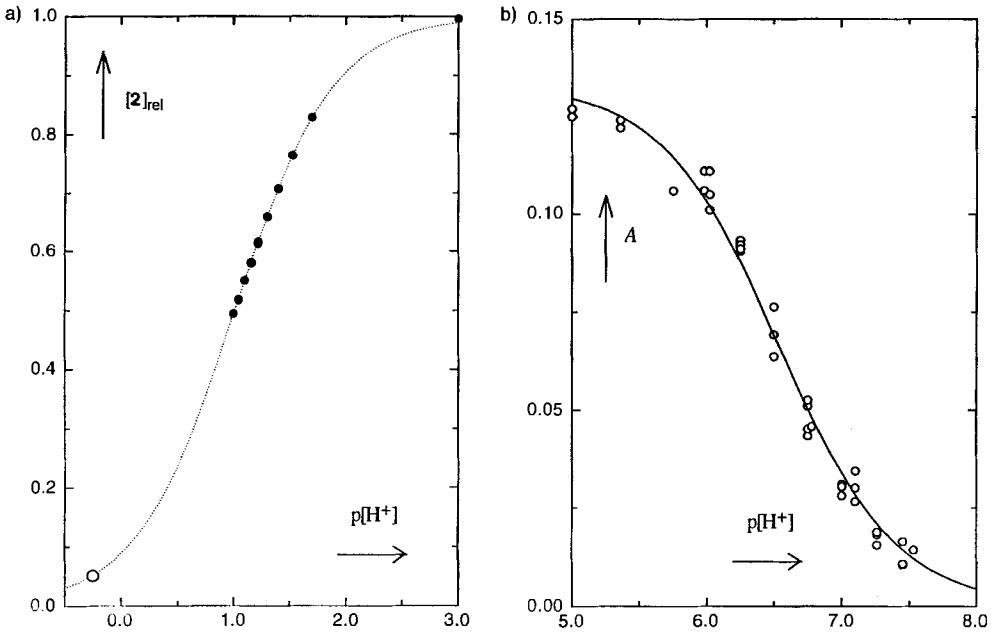

Fig. 6. a) *Spectrophotometric titration of the equilibrium* $\mathbf{2} + H^+ \rightleftharpoons \mathbf{2}^+$. The ordinate is the normalized concentration of **2** as determined by factor analysis. b) *Spectrophotometric titration of the equilibrium* $\mathbf{2} \rightleftharpoons \mathbf{2}^- + H^+$. The ordinate is the initial transient absorbance at 610 nm.

respectively. Combination of these results with the rate constants determined in HCl/H_2O and $HClO_4/H_2O$ at exactly matching concentrations (three measurements each) gave an inverse kinetic isotope effect of $k_{(H^+)}/k_{(D^+)} = 0.49 \pm 0.01$.

Discussion. – Rate and equilibrium constants determined in this work are summarized in *Table 3*. We now address the three questions posed in the introduction sequentially.

Table 3. *Rate and Equilibrium Constants* (aqueous solutions, 25°)

Symbol	Reaction	Value
k_0	$\mathbf{2}^+ + H_2O \rightarrow \mathbf{3}$ (X = OH)	$(9.4 \pm 0.8) \times 10^7\ s^{-1}$
$k_{(N_3^-)}$	$\mathbf{2}^+ + N_3^- \rightarrow \mathbf{3}$ (X = N_3)	$(1.03 \pm 0.14) \times 10^{10}\ M^{-1}\ s^{-1}$
$k_{(HCO_2^-)}$	$\mathbf{2}^+ + HCO_2^- \rightarrow \mathbf{3}$ (X = HCO_2)	$(1.25 \pm 0.42) \times 10^8\ M^{-1}\ s^{-1}$
k_{en}	$S_1(\mathbf{1}) \rightarrow \mathbf{2}$	$\geq 5 \times 10^{11}\ s^{-1}$
k_{ket}	$\mathbf{2} \rightarrow \mathbf{1}$	$\leq 1 \times 10^4\ s^{-1}$
$k_{(H^+)}$	$\mathbf{2} + H^+ \rightarrow \mathbf{2}^+$	$(1.6 \pm 0.5) \times 10^{10}\ s^{-1}$
$pK_a(\mathbf{2}^+)$[a]	$\mathbf{2}^+ \rightleftharpoons \mathbf{2} + H^+$	1.08 ± 0.04
$pK_a(\mathbf{2})$[a]	$\mathbf{2} \rightleftharpoons \mathbf{2}^- + H^+$	6.45 ± 0.04
$pK_a(\mathbf{1}^+)$	$\mathbf{1}^+ \rightleftharpoons \mathbf{1} + H^+$	*ca.* -8
pK_E	$\mathbf{1} \rightleftharpoons \mathbf{2}$	*ca.* 18[b])

[a]) These acidity constants are ionization quotients determined at ionic strength $I = 0.1$M.
[b]) Calculated, see *Table 4*.

Mechanism of Photoenolization. We had concluded earlier [1] that the rate of photoenolization of **1** exceeds 10^9 s^{-1}. With the improved time resolution of the pump-probe apparatus available in this work (excitation with a 800-fs pulse at 248 nm), we find that enol **2** is formed in the ground state within 2 ps of excitation. The absorbance changes observed during the first ps probably reflect thermalization of vibrationally excited enol rather than the enolization process itself. The rate of intersystem crossing of parent 1,4-naphthoquinone in MeCN solution is $(1.1 \pm 0.2) \times 10^{11}$ s^{-1}. *We conclude that enolization from the excited singlet state of* **1** *is too rapid for intersystem crossing to compete.*

In the photoenolization of the related ketone 3,3,6,8-tetramethyl-1-tetralone, intersystem crossing and H transfer from the singlet state were found to be about equally efficient [4]. Besides fast photoenolization (≤ 20 ns) from the singlet state, additional enol was formed in a time-resolved process. The reaction from the excited triplet state proceeded adiabatically to the triplet state of the enol that decayed on a μs time scale. Such behavior is predicted by a state correlation diagram; the analysis given earlier [4] applies directly to the photoenolization of **1**. The singlet reaction is predicted to produce directly the enol ground state. Photoenolization from the triplet state of **1** should yield enol **2** adiabatically in its triplet state. The fact that the ground-state absorption of photoenol **2** develops fully within a few ps is, therefore, strong evidence that photoenolization takes place predominantly, if not exclusively, from the excited singlet state of **1**. The high rate suggests that *photoenolization of singlet excited* **1** *to the ground state of* **2** *is an adiabatic reaction proceeding by passage through a conical intersection* [15] *of the lowest singlet hypersurfaces* S_0 *and* S_1.

Rate-Determining Step in the Photohydration of **1**. We first recall a few experimental facts from the previous work [1]. Photoenolization of 5-methyl-1,4-naphthoquinone (**1**) is efficient in all solvents investigated. In aprotic solvents, intramolecular reketonization of the photoenol **2** dominates: the quantum yield of disappearance of **1** is less than 10^{-3} in, *e.g.*, dry benzene. The rate of intramolecular reketonization depends strongly on solvent polarity, in particular on the H-bond acceptor properties of the solvent; it increases from 10^1 s^{-1} in HMPA to 10^5 s^{-1} in cyclohexane. A bilinear regression of the reketonization rates observed in aprotic media *vs.* the *Taft-Kamlet* solvent parameters π^* and β [16] gives the relation $\log(k_{(\mathbf{2} \rightarrow \mathbf{1})}/s^{-1}) = 4.84 - 1.27\pi^* - 2.47\beta$, from which the rate constant of intramolecular reketonization in H_2O is estimated as 1×10^3 s^{-1}.

The observed decay rates of **2** are well above the estimated rate for intramolecular reketonization. Reketonization to **1**, be it by proton transfer from the solvent to the methylidene group or by intramolecular [1,5]-H-transfer, is not an important contribution to the decay of enol **2** in aqueous solution, because the quantum yield of disappearance of **1** is unity in acidic aqueous solutions, where the hydrate **3** (X = OH) is formed, and rises to *ca.* 2 in neutral and basic solutions, where enolate $\mathbf{2}^-$ reacts with remaining quinone **1**. *Photoenolization is an irreversible process in aqueous solution at all pH values.*

It was proposed [1] that oxygen protonation, $\mathbf{2} + H^+ \rightarrow \mathbf{2}^+$, was the rate-determining step in the photosolvolysis of **1** in AcOH, and that the resulting benzylic cation $\mathbf{2}^+$ then combined with AcO^- ion in a rapid subsequent step. That unusual proposal was put forward because the addition of AcONa to the glacial AcOH medium did not influence the lifetime of **2**, whereas traces of mineral acid quenched it without affecting the efficiency of the overall reaction **1** → **3**. Oxygen-to-oxygen proton transfer such as $\mathbf{2} + H^+ \rightarrow \mathbf{2}^+$, however, is generally very fast, whereas bond formation between heavy

atoms such as the reaction $\mathbf{2}^+ + X^- \rightarrow \mathbf{3}$ is usually slower. It is likely, moreover, that the addition of AcONa would have reduced the acidity of the reaction medium and consequently lowered the concentrations of $\mathbf{2}^+$. Then, if $\mathbf{2}^+$ had formed by rapid pre-equilibrium rather than rate-determining protonation of **2**, its concentration would have been lowered, and that might have offset the accelerative effect of increased AcO^- ion concentration on the nucleophilic capture of $\mathbf{2}^+$

Four pieces of evidence reported in this work consistently show that the protonation equilibrium $\mathbf{2} + H^+ \rightleftharpoons \mathbf{2}^+$ is established rapidly and that, contrary to the earlier proposal [1], the rate-determining step of enol trapping is the addition of a nucleophile to the cationic methylidene group of $\mathbf{2}^+$ (*Scheme 1*). First, the solvent isotope effect determined for trapping of **2**, catalyzed by the hydronium ion, is strongly inverse, $k_{(H^+)}/k_{(D^+)} = 0.49$. This is good evidence for a reaction mechanism in which hydron transfer occurs in a rapidly established equilibrium before the rate-determining step. A mechanism in which hydron transfer is itself rate-determining, on the other hand, would produce an isotope effect in the normal direction ($k_{(H^+)}/k_{(D^+)} > 1$) [17].

Second, the observed saturation of acid catalysis at acid concentrations around 0.1M (*Fig. 5*) reinforces the proposal that protonation of **2** reaches a pre-equilibrium. This indicates that the position of the pre-equilibrium protonation shifts from enol **2** to its conjugate acid $\mathbf{2}^+$; the substrate will then be largely in its reactive protonated form, and a further increase in acid concentration will no longer enhance the reaction rate. If, on the other hand, the H^+ transfer step itself were rate-determining, no such saturation of acid catalysis would occur. With this interpretation, the saturation of acid catalysis defines the acid dissociation constant of the carbonyl-protonated enol $\mathbf{2}^+$. Analysis of the kinetic data by *Eqn. 2* gave $pK_a = 1.10 \pm 0.05$ ($I = 0.1$M).

Third, the pre-equilibrium protonation directly manifests itself by the spectral change of the transient photoenol in acidic solutions (*Fig. 2*). A titration curve fits well to the relative concentrations of **2** determined by factor analysis of the transient spectra in acidic solutions (*Fig. 6, a*). The acidity constant thus determined, $pK_a(\mathbf{2}^+) = 1.01 \pm 0.10$, is consistent with that determined independently from the kinetic data. Conjugate acids of aromatic ketones are generally much more acidic than this; for example, $pK_a = -4.7$ was reported for protonated benzophenone [18]. The high basicity of the carbonyl group in **2** is, however, not unprecedented: other protonated quinone methides, such as fuchsone [19] and diphenylquinocyclopropene [20], have similarly high pK_a values, which were rationalized on the basis of semiempirical SCF-MO calculations [21]. Based on similar calculations (*Exper. Part, Eqn. 5*), we estimate the $pK_a(\mathbf{2}^+)$ as 1.2 ± 0.9 in good agreement with the experimental value. Qualitatively, the low acidity of protonated quinone methides arises from charge delocalization onto the exocyclic methylidene C-atom and rearomatization of the naphthyl system, as indicated in the resonance structure shown for $\mathbf{2}^+$ in *Scheme 1*. Charge delocalization to the methylidene group also manifests itself in the high reactivity of $\mathbf{2}^+$ towards water, $k_0 = (9.4 \pm 0.8) \times 10^7\ s^{-1}$. Note, however, that genuine benzyl cations are even more reactive towards H_2O [22].

Lastly, a pre-equilibrium proton-transfer mechanism is also consistent with the behavior in buffer solutions, whereas a rate-determining proton-transfer mechanism is not. If proton transfer were rate-determining, the slopes of the buffer dilution plots would represent specific rate constants for the proton-transfer step, and these should increase in magnitude with increasing acid strength of the proton donor. That, however, is not

the case: the slope of the HN_3 buffer dilution plot is an order of magnitude greater than that of the HCO_2H plot, 4.4×10^6 *vs.* 4.3×10^5 M^{-1} s^{-1}, respectively, and yet HN_3 is by far the weaker acid, $pK_a^{\ominus}(HN_3) = 4.65$ *vs.* $pK_a^{\ominus}(HCO_2H) = 3.75$. With the mechanism of azide addition shown in *Scheme 1*, the bimolecular rate constant for azide addition to $\mathbf{2}^+$ may be calculated from the slope of the buffer dilution plot: $k_{(HN_3)} = k_{(N_3^-)} \times K_a(HN_3)/K_a(\mathbf{2}^+)$; $k_{(N_3^-)} = (1.03 \pm 0.14) \times 10^{10}$ M^{-1} s^{-1}. The addition of azide, a much stronger nucleophile than H_2O, is essentially diffusion-controlled and about two orders of magnitude faster than the addition of formate (*Table 3*). *These experimental observations leave no doubt that nucleophilic trapping of* $\mathbf{2}^+$ *by* H_2O *is rate-determining in the acid-catalyzed hydration of* **2**.

Picosecond flash photolysis provides absolute values for the rate constants of interest here (*Eqn. 1*). The protonation reaction of **2** may be treated as a pre-equilibrium, if the deprotonation of $\mathbf{2}^+$ is much faster than the nucleophilic addition of H_2O, $k_{(-H^+)} \gg k_0$. The rate of protonation of $\mathbf{2}^+$, $k_{(H^+)}$, and the acidity constant $K_a(\mathbf{2}^+)$ are both known, hence the rate of deprotonation is $k_{(-H^+)} = k_{(H^+)} \times K_a(\mathbf{2}^+) = (1.6 \pm 0.5) \times 10^{10}$ M^{-1} $s^{-1} \times (0.083 \pm 0.007)M = (1.3 \pm 0.4) \times 10^9$ s^{-1}. This is indeed more than an order of magnitude faster than the nucleophilic addition of H_2O to $\mathbf{2}^+$, $k_0 = (9.4 \pm 0.8) \times 10^7$ s^{-1}.

Oxygen vs. *Carbon Protonation of* **2**. The standard reaction enthalpy of enolization $\mathbf{1} \rightarrow \mathbf{2}$ was calculated by three semiempirical methods (AM1, AM1-SM2, and PM3) and using *Benson*'s increments [23][1]). The results are collected in *Table 4*. Taking an average value of 100 kJ mol^{-1} for the enthalpy of enolization and ignoring entropy contributions, the enolization constant is estimated as $pK_E \equiv -\log([\mathbf{2}]/[\mathbf{1}]) \approx 18$. The pK_a reported for carbonyl-protonated naphthoquinone is -7.2 [24]; it is, however, not clear whether the correct acidity function was used to analyze the data. We observed half-protonation of **1** in very concentrated H_2SO_4 solutions, $H_0 \approx -9$. Based on the semiempirical calculations described in the *Exper. Part* (*Eqn. 5*), we estimate $pK_a(\mathbf{1}^+) = -7.6 \pm 0.8$. Assuming a value of $pK_a(\mathbf{1}^+) \approx -8$, the upper thermodynamic cycle shown in *Scheme 2* then gives $pK_a \approx 10$ for ionization of the protonated quinone as a carbon acid to give enol, $\mathbf{1}^+ \rightarrow \mathbf{2}$. Hence, protonation of enol **2** on carbon, $\mathbf{2} \rightarrow \mathbf{1}^+$, is thermodynamically favored over protonation on oxygen, $\mathbf{2} \rightarrow \mathbf{2}^+$, by roughly 9 pK units or 50 kJ mol^{-1}. The thermodynamic bias for *C*-protonation is even stronger for the enolate $\mathbf{2}^-$ (lower cycle shown in *Scheme 2*): it is equal to the free energy of enolization, *i.e.*, about 100 kJ mol^{-1}. Nevertheless, *C*-protonation is, at most, a minor side reaction

Table 4. *Calculated Enthalpies of Formation of* **1** *and* **2**

Method	$\Delta_f H_m^{\ominus}$(**1**, 298 K)/kJ mol^{-1}	$\Delta_f H_m^{\ominus}$(**2**, 298 K)/kJ mol^{-1}	$\Delta_r H_m^{\ominus}$(**1** → **2**, 298 K)/kJ mol^{-1}
AM1 [27]	−91	9	100
AM1-SM2 [28][a])	−114	−30	84
PM3 [29]	−122	−8	114
Benson [23]	−144	−30	114

[a]) The AM1-SM2 model is designed to include aqueous solvation free energies.

[1]) The increment $O-(C_d)H = -202$ kJ mol^{-1} was taken from [23b].

at all pH values, since the quantum yield of photohydration is unity in acidic solutions and rises to two in basic solutions. *C*-Protonation of **2** or $\mathbf{2}^-$ amounts to reketonization of the photoenol and would show up as inefficiency of the photoreaction and by D incorporation from D_2O. *Thus, the protonation of both* $\mathbf{2}^-$ *and* **2** *is kinetically controlled; C-protonation does not compete with O-protonation despite a substantial thermodynamic bias in favor the former.* This is remarkable in view of the extremely rapid H-transfer from the C- to the O-atom that takes place upon photoenolization of singlet excited **1**.

Scheme 2

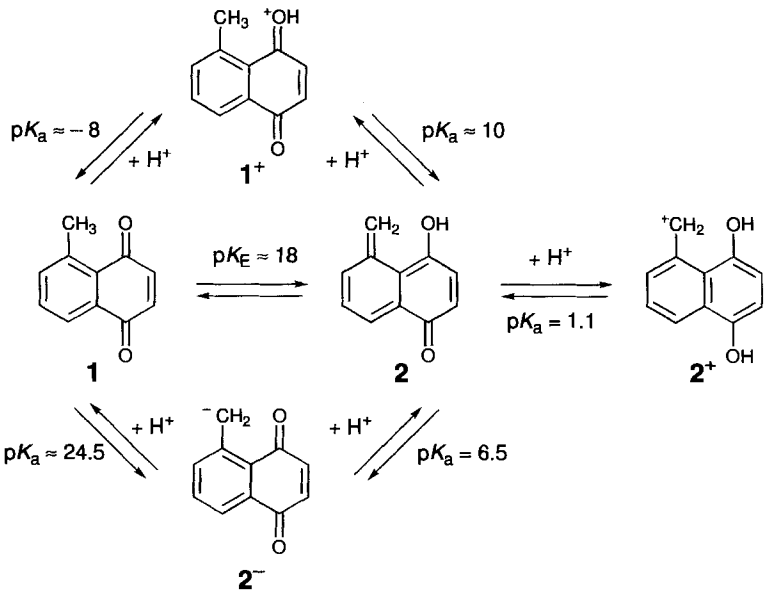

This work was supported by the *Swiss National Science Foundation*. *Y.C.* and *A.J.K.* thank the *Natural Sciences and Engineering Research Council of Canada* for a travel grant.

Experimental Part

Materials. 5-Methyl-1,4-naphthoquinone (**1**) was available from the previous investigation [1] and was repurified by recrystallization from hexane giving yellow needles. M.p. 119–120° ([25]: 122–123°). All other materials were best available commercial grades.

Identification of Photoproduct **3** (X = OH). A soln. of 10 mg of **1** in a mixture of 10 ml of 0.01N aq. $HClO_4$ and 1 ml of MeCN was irradiated for 1 h through a cut-off glass filter ($\lambda > 370$ nm) with a high-pressure Hg arc (*Osram HBO* 200 W) until the UV spectrum of an aliquot indicated complete conversion (*Fig. 1*). The photoproduct was reasonably stable in aq. acid, but could not be isolated in pure form. It slowly oxidized in air, and dehydrated upon workup or injection into a gas chromatograph equipped with a 5% phenyl-methyl silicon column (injection chamber temp. 100°, column temp. 270°), such that GC/MS analysis indicated only the presence of starting material **1** (173 (15), 172 (100, M^+), 144 (25, $[M-CO]^+$), 115 (80, $[M-CO, -CHO]^+$)), and small amounts of an oxidation product, presumably 5-(hydroxymethyl)-1,4-naphthoquinone (188 (100, M^+)), despite the fact that UV monitoring had indicated complete conversion of **1** to **3** (X = OH). ^{1}H-NMR Spectra of **3** (X = OH) were determined from samples irradiated in degassed aq. acid and extracted with $CDCl_3$. Drying (Na_2SO_4 or molecular sieves) was avoided since it accelerated dehydration of **3** (X = OH) to **1**. Nevertheless, all

samples contained various decomposition products that commonly contributed more than half of the integrated intensity.

Quantum-Yield Determinations. The amount of conversion was determined spectro-photometrically, and the amount of light absorbed in the quartz cell was determined by azobenzene actinometry [26]. The light source was a stabilized medium-pressure Hg arc equipped with a band-pass filter transmitting at 365 nm. The extinction coefficient of **1** in aq. soln. (with 1% MeCN) at 365 nm, $\varepsilon = 3180 \pm 100\text{M}^{-1}\,\text{cm}^{-1}$, was measured by diluting an MeCN stock soln. of **1** with H_2O. Five series of independent quantum-yield measurements with *ca.* 30 intermediate readings each were done for acid concentrations of 0.001, 0.01, and 1.00M $HClO_4$ that gave average values of $\phi_{hydr} = 0.93 \pm 0.10$, 1.00 ± 0.04, and 1.00 ± 0.10, respectively.

Flash Photolysis. The three setups for the different time scales of ps, ns, and μs have been described in [9]. Nanosecond kinetic and spectrographic flash photolysis was performed by excitation with 20-ns pulses from an excimer laser operated with XeF (351 nm) or KrF (248 nm). A 248 nm excitation pulse of 0.8-ps duration was used to study short-lived phenomena by pump-probe absorption spectroscopy. The decay kinetics observed with acidic solns. conformed to the first-order rate law well, and the corresponding rate constants were obtained by nonlinear least-squares fitting of a single exponential function to the digitized decay traces. Traces obtained with neutral or weakly basic solns. indicated contributions from a second-order process. Most experiments were carried out with aerated solns. that were kept at $25 \pm 1°$. Control experiments with degassed solns. were carried out for various pH, but in no case did the presence of air affect the transient kinetics.

Semiempirical Calculations. Heats of formation (*Table 4*) were calculated by the methods AM1 [27], AM1-SM2 [28], and PM3 [29] as provided in the MacSpartan *plus* software package (version 1.0, 1996). Geometries were fully optimized in each model. The AM1-SM2 model is parametrized to include aq. solvation free energies. This model was used to calculate ionization energies for the protonated ketones and aldehydes given in *Table 5*. Linear regression, treating the calculated values as the independent variable, gave the relation

$$pK_{a,\text{calc.}} = (-3.47 \pm 0.36) + (0.101 \pm 0.012)[\Delta E_{\text{calc.}}/(\text{kJ mol}^{-1}) + 485.8] \quad (5)$$

from which the pK_a values of $\mathbf{1}^+$ and $\mathbf{2}^+$ were estimated. The second constant term is the sample mean of the calculated proton affinities in units of kJ mol^{-1}.

PPP SCF SCI Calculations [30] were done to predict the electronic absorption spectra of photoenol **2**, its conjugate acid $\mathbf{2}^+$, and its conjugate base $\mathbf{2}^-$. Idealized geometries were assumed (bond lengths 140 pm, bond

Table 5. *Calculated Ionization Energies* (AM1-SM2) *and* pK_a *Values for Various Protonated Ketones and Aldehydes*

Compound	$\Delta E/(\text{kJ mol}^{-1})$	pK_a	Ref.
Benzaldehyde	−500.3	−4.48	[18]
Naphthalene-2-carbaldehyde	−501.9	−6.68	[21]
9*H*-Fluoren-9-one	−523.7	−6.65	[21]
Phenanthrene-9-carbaldehyde	−503.7	−6.34	[21]
Naphthalene-1-carbaldehyde	−505.1	−6.34	[21]
Anthracene-1-carbaldehyde	−490.6	−5.71	[21]
Anthracene-9-carbaldehyde	−507.6	−4.81	[21]
Benzophenone	−508.0	−4.71	[18]
Acetophenone	−512.4	−3.87	[18]
Acetone	−482.7	−3.08	[18]
2,3-Diphenylcyclopropen-1-one	−504.9	−3.20	[21]
Perinaphthenone	−471.0	−1.40	[21]
Azulene-1-carbaldehyde	−454.7	−1.00	[21]
Tropone	−446.8	−0.60	[21]
4,4-Diphenyl-1,4-benzoquinone methide (fuchsone)	−449.4	1.70	[21]
1,2-Diphenylquinocyclopropene	−410.6	5.00	[21]
5-Methyl-1,4-naphthoquinone (**1**)	−526.6	(*ca.* −8)[a]	this work
4-Hydroxy-5-methylidenenaphthalen-1(5*H*)-one (**2**)	−440.0	(1.1)[a]	this work

[a]) Not included for linear regression.

angles 120°) and standard parameters were used [1]: valence state ionization potentials $I_\mu \equiv 0$ eV for carbon (−21.48 and −2.18 eV for −OH and =O, resp.), one-center repulsion integrals $\gamma_{\mu\mu} = 10.84$ eV (22.9 and 11.3 eV for OH and =O, resp.), core resonance integrals $\beta_{\mu\nu} = -2.318$ eV, core charges $Z^c = 1$ (2 for −OH), two-center repulsion integrals $\gamma_{\mu\nu} = 1439.5/(132.8 + R_{\mu\nu}/\text{pm})$ eV. All singly excited configurations were included for CI.

REFERENCES

[1] E. Rommel, J. Wirz, *Helv. Chim. Acta* **1977**, *60*, 38.
[2] M. Chatterjee, S. E. Rokita, *J. Am. Chem. Soc.* **1990**, *112*, 6397; *ibid.* **1991**, *113*, 5116; *ibid.* **1994**, *116*, 1690.
[3] N. P. Gritsan, I. V. Khmelinski, O. M. Usov, *J. Am. Chem. Soc.* **1991**, *113*, 9615; N. P. Gritsan, L. S. Klimenko, *J. Photochem. Photobiol. A* **1993**, *70*, 103.
[4] R. Haag, J. Wirz, P. J. Wagner, *Helv. Chim. Acta* **1977**, *60*, 2595.
[5] a) H. S. Harned, N. D. Embree, *J. Am. Chem. Soc.* **1934**, *56*, 1042; b) H. S. Harned, R. W. Ehlers, *ibid.* **1933**, *55*, 652.
[6] S. Ahrland, E. Avsar, *Acta Chem. Scand., Ser. A* **1975**, *29*, 881.
[7] R. G. Bates, 'Determination of pH', 2nd edn., Wiley, New York, 1973.
[8] G. J. Fischer, E. J. Land, *Photochem. Photobiol.* **1983**, *37*, 27; I. Loeff, S. Goldstein, A. Treinin, H. Linschitz, *J. Phys. Chem.* **1991**, *95*, 4423.
[9] E. Hasler, A. Hörmann, G. Persy, H. Platsch, J. Wirz, *J. Am. Chem. Soc.* **1993**, *115*, 5400.
[10] G. M. Loudon, *J. Chem. Educ.* **1991**, *68*, 973.
[11] H. Gampp, M. Maeder, C. J. Meyer, A. D. Zuberbühler, *Talanta* **1985**, *32*, 95; M. Maeder, A. D. Zuberbühler, *Anal. Chem.* **1990** *62*, 20220.
[12] H. Sigel, A. D. Zuberbühler, O. Yamauchi, *Anal. Chim. Acta* **1991**, *255*, 63.
[13] H. S. Harned, R. W. Ehlers, *J. Am. Chem. Soc.* **1933**, *33*, 652.
[14] A. K. Grzybowski, *J. Phys. Chem.* **1958**, *62*, 555.
[15] F. Bernardi, M. A. Robb, M. Olivucci, *Chem. Soc. Rev.* **1996**, *24*, 321; M. Klessinger, *Angew. Chem. Int. Ed.* **1995**, *34*, 549.
[16] M. J. Kamlet, J. L. M. Abboud, R. W. Taft, *Progr. Phys. Org. Chem.* **1981**, *13*, 485.
[17] J. R. Keefe, A. J. Kresge, 'Techniques of Chemistry, Volume VI, Investigation of Rates and Mechanisms of Reactions', Ed. C. F. Bernasconi, Wiley-Interscience, New York, 1968, Part I, Chapt. XI.
[18] A. Bagno, G. Scorrano, R. A. More O'Ferrall, *Rev. Chem. Interm.* **1987**, *7*, 313; A. Bagno, V. Lucchini, G. Scorrano, *J. Phys. Chem.* **1991**, *95*, 345.
[19] A. Kende, *J. Am. Chem. Soc.* **1963**, *85*, 1882.
[20] L. Zucker, L. P. Hammett, *J. Am. Chem. Soc.* **1939**, *61*, 2779.
[21] M. J. S. Dewar, T. Morita, *J. Am. Chem. Soc.* **1969**, *91*, 802.
[22] J. P. Richard, *Tetrahedron* **1995**, *51*, 1535.
[23] a) S. W. Benson, F. R. Cruickshank, D. M. Golden, G. R. Haugen, H. E. O'Neal, A. S. Rodgers, R. Shaw, R. Walsh, *Chem. Rev.* **1969**, 279; b) F. Tureček, Z. Havlas, *J. Org. Chem.* **1986**, *51*, 4066.
[24] T. Handa, *Bull. Chem. Soc. Jpn.* **1955**, *28*, 483.
[25] E. R. H. Jones, H. H. Lee, M. C. Whiting, *J. Chem. Soc.* **1960**, 341.
[26] G. Gauglitz, S. Hubig, *Z. Phys. Chem. N.F.* **1984**, *139*, 237; G. Gauglitz, S. Hubig, *J. Photochem.* **1985**, *30*, 121. G. Persy, J. Wirz, *EPA Newslett.* **1987**, *11*, 685.
[27] M. J. S. Dewar, E. G. Zoebisch, E. F. Healy, J. P. P. Stewart, *J. Am. Chem. Soc.* **1985**, *107*, 3908.
[28] C. J. Cramer, D. G. Truhlar, *J. Am. Chem. Soc.* **1991**, *113*, 8305; C. J. Cramer, D. G. Truhlar, *Science* **1992**, *256*, 213; C. J. Cramer, D. G. Truhlar, *J. Computer Aided Molecular Design* **1992**, *6*, 69.
[29] J. J. R. Stewart, *J. Computer Aided Molecular Design* **1990**, *4*, 1.
[30] R. Pariser, R. G. Parr, *J. Chem. Phys.* **1953**, *21*, 466; J. A. Pople, *Trans. Faraday. Soc.* **1953**, *49*, 1375.